SAE INTERNATIONAL

ARTICLE INFO
Article ID: 03-17-05-0037

doi:10.4271/03-17-05-0037

Water Droplet Collison and Erosion on High-Speed Spinning Wheels

Richárd Takács,[1] Ibolya Zsoldos,[2] and Dániel Szentendrei[2]

[1]Széchenyi István University, Audi Hungaria Faculty of Automotive Engineering, Department of Propulsion Technology, Hungary
[2]Széchenyi István University, Hungary

Abstract

The water droplet erosion (WDE) on high-speed rotating wheels appears in several engineering fields such as wind turbines, stationary steam turbines, fuel cell turbines, and turbochargers. The main reasons for this phenomenon are the high relative velocity difference between the colliding particles and the rotor, as well as the presence of inadequate material structure and surface parameters. One of the latest challenges in this area is the compressor wheels used in turbochargers, which has a speed up to 300,000 rpm and have typically been made of aluminum alloy for decades, to achieve the lowest possible rotor inertia. However, while in the past this component was only encountered with filtered air, nowadays, due to developments in compliance with tightening emission standards, various fluids also collide with the spinning blades, which can cause mechanical damage. One such fluid is the condensed water in the low-pressure exhaust gas recirculation channel (LP-EGR) formulated at cold starts and low-speed high load conditions. This kind of design has been developed to reduce nitrogen oxide emissions and is used in both gasoline and diesel engines. This article presents a state-of-the-art review of this WDE process, focusing on the formation of the condensed water before the compressor wheel, summarizing the influencing factors of WDE and the effects of the damage including using component testbench experiences and simulation methodologies. Inspection possibilities such as high-speed camera measurement and vibration analysis are also an important part of the document.

History

Received: 20 Sep 2023
Revised: 28 Nov 2023
Accepted: 14 Mar 2024
e-Available: 04 Apr 2024

Keywords

Water droplet erosion,
Compressor wheel,
Vibration, Material structure

Citation

Takács, R., Zsoldos, I., and Szentendrei, D., "Water Droplet Collison and Erosion on High-Speed Spinning Wheels," *SAE Int. J. Engines* 17(5):653-667, 2024, doi:10.4271/03-17-05-0037.

ISSN: 1946-3936
e-ISSN: 1946-3944

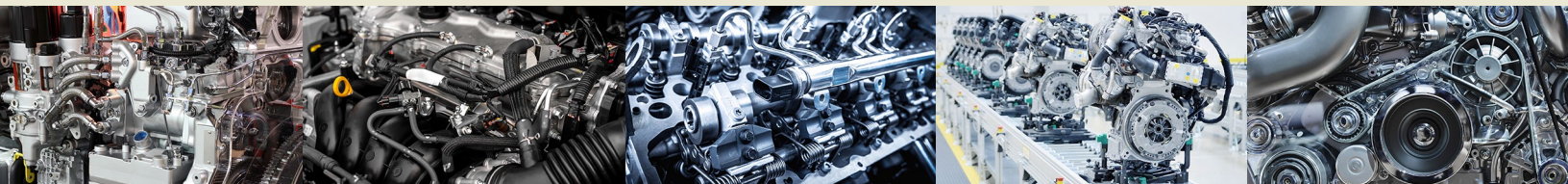

1. Introduction

While the automotive industry is increasingly focusing on the development of electric drivetrains, mainly because of their zero local exhaust emission, there are several arguments in favor of further development of internal combustion engines. One argument is the recent widespread use of life-cycle CO_2 emission assessment, which, according to the research of Del Pero et al. [1], shows that the balance is only tipping in favor of electric powertrains when electricity is generated from renewable sources. However, the renewable sources are barely 8.5% of the global energy mix, as observed in Figure 1 [2] without a medium-term forecast of significant increase.

A further argument is the increasing use of hybrid vehicles, a type of drivetrain with an internal combustion engine optimized for a narrower speed range, thus with lower consumption and emissions, but with a longer range than a pure electric vehicle. It is also worth considering the area of commercial vehicles, heavy machinery, ships, and stationary engines where the size of the masses to be moved, or the high-power levels required for operation, may not make it economical to develop electric drivetrains according to Serrano et al. [3]. In these areas, it is assumed that turbocharged diesel engines will continue to prevail and maybe evolve into H_2-propelled combustion engines.

However, in addition to CO_2 emission reduction, a selection of additional requirements must be met at the production of ICEs. One of these is the reduction of nitrogen oxide emissions, which is the greatest challenge of nowadays' development. According to the latest European legislation, EUR6d ISC-FCM [4], the maximum NO_x emissions for passenger car diesel engines manufactured after January 1, 2021, must be less than 80 mg/km, while for petrol engines the maximum NO_x emissions is 60 mg/km [5]. Similar targets exist in the US, where the government aims to reduce NO_x emissions by 90% between 2010 and 2024 [6]. This difficult development challenge may be further compounded in some areas using biodiesel as an alternative fuel, while these fuels generate more NO_x due to their longer HC chains, which result in higher O_2 content [7]. Even soy, rapeseed, and palm as a fuel contains 4–8% higher amount of water [8].

An effective and now widely used solution is to recirculate a certain amount of exhaust gas back into the cylinders, either by means of valve control (internal EGR) or by means of an external actuator (external EGR) to return it to the intake manifold.

Bermúdez et al. [9] provided concrete figures on the benefits of this combined system using engine testbench measurements. By adapting the engine management to this hybrid feedback system, up to 21% NO_x emission and 8.5% fuel consumption reduction can be realized during a New European Driving Cycle (NEDC) (2.0 l high-speed, direct-injected (HSDI) engine).

In both cases, when the same power level is reached, a higher mass of charge is present in the cylinders, the heating of which removes heat from the thermal cycle, reducing the peak combustion temperature and thus NO_x emissions [10, 11]. In the case of gasoline engines, exhaust gas recirculation (especially at part load) is also associated with a reduction in consumption, as explained by Jung et al. [12] The same power level to be maintained at increased charge requires a larger throttle opening, thus reducing throttle loss. Several solutions have been developed to achieve the emission requirements mentioned above. Initially, high-pressure exhaust gas recirculation (HP-EGR) installed between the exhaust ports and the turbine was used, which drives a given amount of the exhaust gases into the intake manifold section downstream of the compressor (Figure 2). However, the requirement to reduce nitrogen oxides to an ever-increasing extent required the recirculation of more and more exhaust gas at increasing charge pressures, which could not be fulfilled with HP-EGR due to the pressure conditions. In 2008, this led to the introduction of low-pressure recirculation, in which exhaust gas is fed from the outlet of the particle filter to the turbocharger's compressor intake side (Figure 2). Serrano et al. [13] listed the following advantages and disadvantages of using this system.

FIGURE 1 Evolution of world energy consumption by origin during the last 21 years. Data taken from Ref. [2].

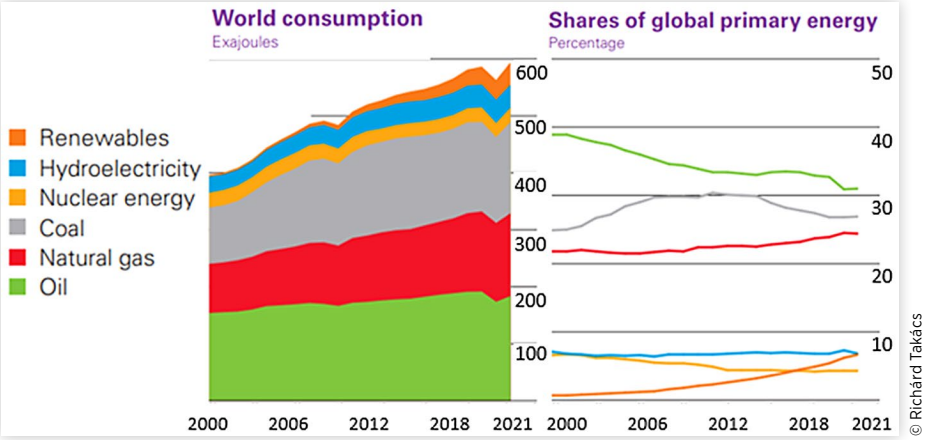

FIGURE 2 Schematic of a hybrid EGR system.

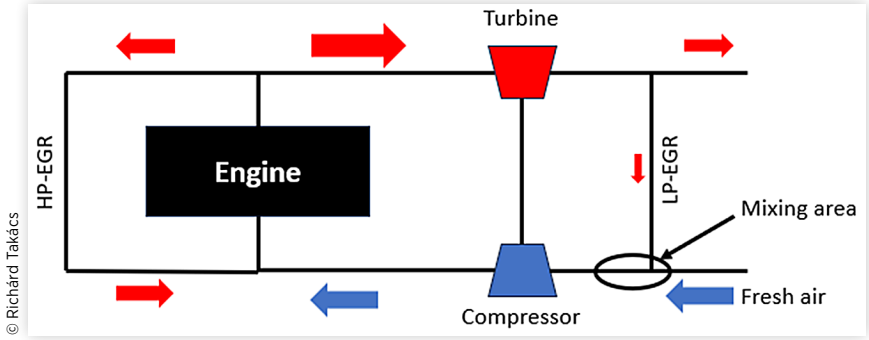

Advantages:

- There is no mass flow reduction on the turbine, thus:
  - No decrease in performance
  - Better gas response due to faster reach of boost pressure
- Lower charge air temperature
- There is more time for the gases to mix before they enter the cylinder, so referring to [7], hence the charge of each cylinder shows a much more homogeneous picture

Disadvantages:

- Expensive design due to increased part count
- Increased control response time due to longer channels
- The accumulated water condensate can mechanically damage the compressor blades

Desantes et al. [14] mentioned the effect of backpressure downstream the particulate filter, or a throttle valve upstream of the compressor, which serves to maintain pressure differentials between the channels while increasing throttling/pumping losses as a further drawback. Furthermore, Warey et al. [15] cited the risk of clogging of the radiator between the control valve and the intake manifold with particulate matter, as the exhaust gas is recirculated from the particulate filter upstream of the exhaust manifold.

The benefits of combining the two systems and using them as a hybrid control strategy are described in [12] for a full engine characterization field, showing that at higher power points, where high boost pressure is required in addition to recirculated exhaust gas, efficient NO_x reduction can only be achieved by concurrently utilizing the two systems. Figure 3 represents a suggested usage of this hybrid system on a complete engine map.

Siokos et al. [16] defined a characteristic field for the consumption reduction potential of LP-EGR through validated simulations with GT-Power software, which is illustrated in Figure 4. It can be seen, that the lower the engine speed and the higher the brake mean effective pressure the lower the brake specific fuel consumption.

In addition to the control strategy, a separate study was carried out to determine the amount of water condensate at a given operating point (2000 rpm, 4 bar BMEP), considering the amount and temperature of recirculated exhaust gas, and

FIGURE 3 Efficient EGR control strategy over an engine map. Data taken from Ref. [12].

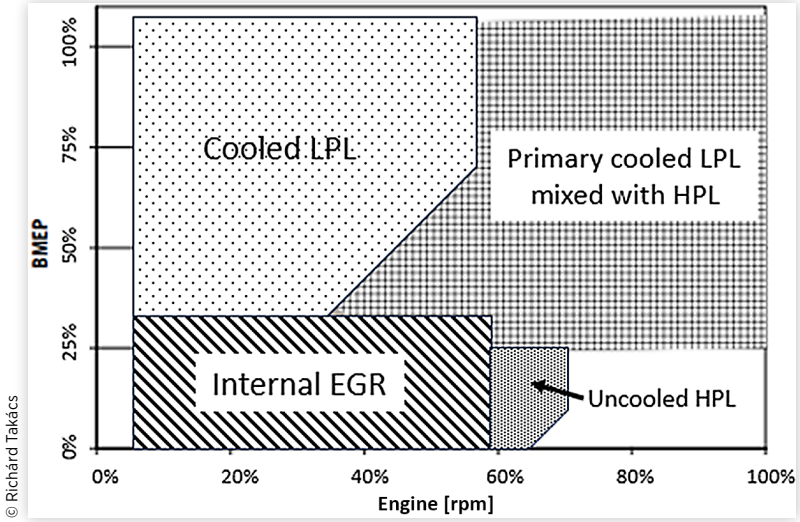

FIGURE 4 Brake specific fuel consumption reduction potentials with optimized LP-EGR strategy. Data taken from Ref. [16].

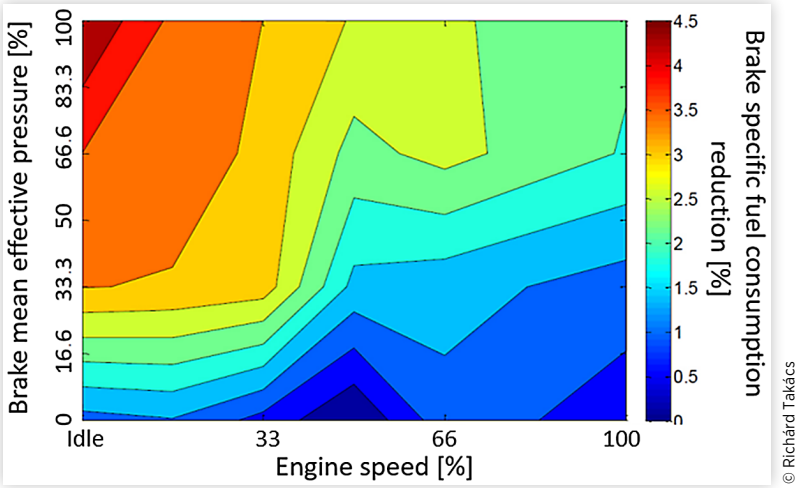

the ambient air temperature. In Figure 5, the negative values represent the condensation.

They concluded that cooling the exhaust gases below 53°C, or operating at ambient temperatures below 0°C with more than 8% EGR would likely lead to water droplet formation.

Dimitriou et al. [17] mentioned another advantage of LP-EGR that it allows a higher mass flow through the turbocharger turbine, which allows the variable turbine geometry to open at a higher angle for the same boost pressure level, resulting in less backpressure and decreased pumping loss (piston displacement work). At low ambient temperatures, high NO_x emissions can also be experienced in the short period after engine start-up until the catalytic converter reaches its operating temperature. To reduce this, Galindo et al. [18] recommended the use of LP-EGR, which allows the intake system to have warmer air compared to the ambient to reach the operating temperature in a shorter period.

The importance of mixing recirculated exhaust gas with the fresh air present in the intake manifold is highlighted in Reihani's research [19]. The short available mixing lengths in HP-EGR applications can cause either misfiring, or the generation of excess unburned hydrocarbons or soot. Through component test bench studies, it has been shown that the geometric quality of the junction between the fresh air upstream of the compressor and the LP-EGR duct, as well as the intensity of the eddy currents present affects the isentropic efficiency of the compressor, the negative effect of which can be counteracted by optimizing the junction angle, length, and diameter.

The use of alternative fuels is one of the most interesting and promising areas of internal combustion engine research

FIGURE 5 Condensation in the function of EGR cooler outlet temperature and ambient air temperature versus EGR mass fraction. Data taken from Ref. [16].

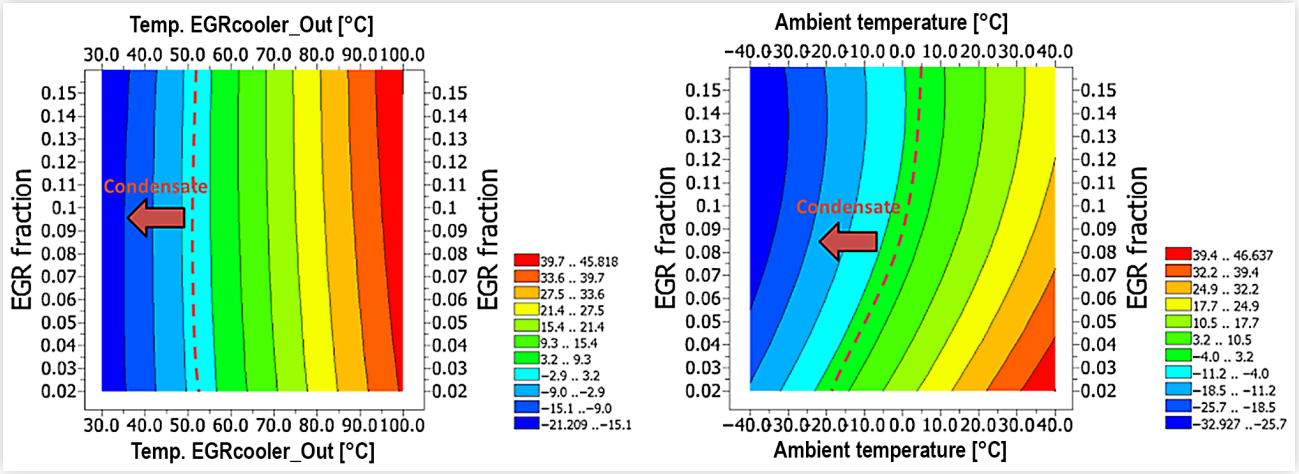

FIGURE 6 Simplified model for LEE investigation. Data taken from Ref. [20].

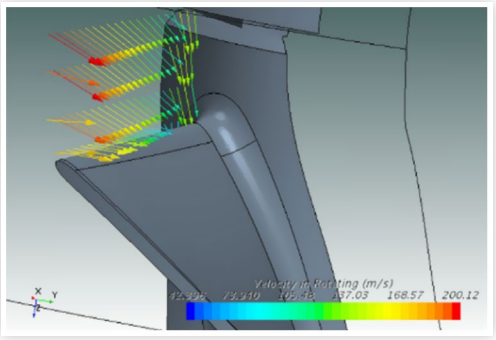

today. The aim is primarily to increase the sustainability of fuel production and to lower CO_2 and pollutant emissions. Yudanov, M. [20] showed that the use of LP-EGR is of great importance for a heavy-duty diesel engine using dimethyl ether fuel, resulting in a design with low CO_2 and NO_x emissions. However, she also realized that this type of fuel can produce even more condensate water having a higher risk of WDE on the leading edge of the spinning compressor wheel (leading edge erosion or LEE). In her simulation methodology, built in StarCCM+ environment, a simplified model to represent this erosion phenomenon was used to reduce the computation times, as shown in Figure 6. This picture represents the relative velocity of spinning wheel compared to the colliding water droplets. It can be seen that the highest difference appears at the outer side of the leading edge. This area has the highest erosion rate in reality, so the author was able to show the root reason for it in a simulation environment.

It can be concluded that the use of LP-EGR has a great potential to reduce the desired NO_x emissions and in some cases fuel consumption, but care should be taken regarding the mentioned disadvantages of the technology.

2. Damaging Effect of Liquid Condensate in Collision with Spinning Wheel

The collision of fluids with moving parts and the resulting wear is a widely investigated research area. In order to understand the basic principle and to determine the effecting factors, several researchers developed methods and hypotheses. Regarding Heymann' theory [21], during the water droplet impact on a solid surface, a shock wave is formed inside the droplet, and it breaks away at a specific moment, then spread toward as lateral jets. During this process, the energy released from the impact pressure transforms to the kinetic energy of lateral jet. Amirzadeh et al. [22] extended this theory with the consideration of the solid surface quality what could create four different erosion mechanism such as direct deformation, stress wave propagation, lateral outflow jetting, or hydraulic penetration. Based on his research, the damage mechanisms during the incubation period are mainly direct deformation and stress wave propagation. However, as the surface roughness is increasing, the lateral jetting and the hydraulic penetration mechanisms are activated (Figure 7).

Li et al. [23] suggested a possible method for lifetime prediction of turbine blades by defining the peak stress from the duration of impact, the impact speed, and the diameter of the droplet. Another key aspect in lifetime prediction is to calculate the rate of erosion of a surface. They build an erosion rate (E) equation as the following formula:

$$E = k\frac{m}{m_{ref}}\left(\frac{V}{V_{ref}}\right)^{\alpha}\left(\frac{d}{d_{ref}}\right)^{\beta} 10^{-(\gamma HV)} \qquad \text{Eq. (1)}$$

where k is the erosion rate constant, m is the droplet mass flow rate, m_{ref} is the reference droplet mass flow rate, V is the

FIGURE 7 Liquid–solid impact, stress and shock wave formation, and possible microcrack/fatigue caused by water drop-solid impact. Data taken from Ref. [23].

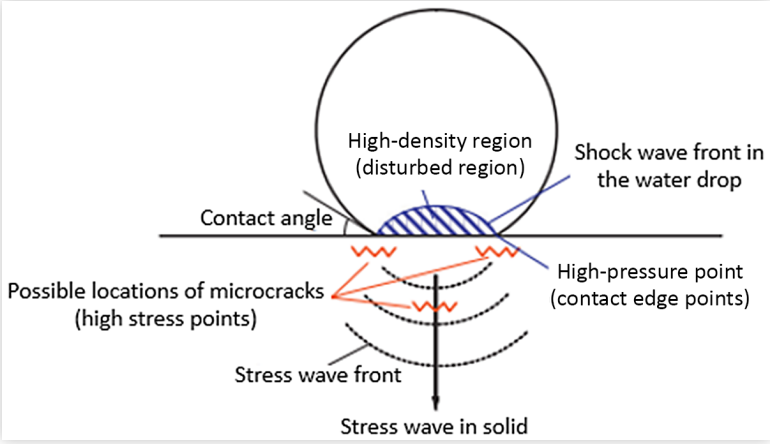

droplet impact velocity, V_{ref} is the reference droplet impact velocity, d is the droplet diameter, d_{ref} is the reference droplet diameter, HV is the Vickers hardness of the base material, and α (5.1), β (2), γ (−0.048) are exponents. Hammitt et al. [24] claimed that the describing factors that determine the level of influence of a liquid droplet impact on a solid surface can be classified into three groups: (a) speed of impact; (b) material and liquid properties; (c) geometrical aspects (angle of impact, surface roughness, shape and size of droplets). There is no complete agreement, but from the viewpoint of material properties and its effect on WDE, some researchers mentioned not just the hardness of the base material, but the ductility, fracture toughness, and fatigue limit too. A deeper study [25] on the effect of the impact angle highlighted the importance of it on incubation time.

To compare different types of methods and approaches for the same purpose, it's essential to define a standard procedure. Most of the time, researchers use the ASTM-G73-10 [26] standard for WDE and leading edge protection investigations.

As it was mentioned earlier, this phenomenon occurs in many engineering fields. Chen et al. [27] and Castorrini et al. [28] conducted simulation studies on wind turbine blades to map the wear patterns (highlighted in Figure 8) and aerodynamic characteristics caused by interacting raindrops. They identify aerodynamic performance loss as a primary consequence and recommend the application of coatings to avoid this phenomenon. Dashtkar et al. [29] detailed various coating techniques, such as sol-gel thin film technique, gelcoat, and polyurethane-based surface coatings, and pointed out that without these, aerodynamic performance loss can be as high as 20–25%.

Erosion mainly affects the leading edge, i.e., the edge of turbine blades facing the rotational direction. The reason for erosion occurring at the leading edge is the magnitude of the peripheral velocity of the rotating blades being the highest, causing the largest velocity difference with respect to the impacting raindrops. A formula is given for the erosion rate, where the extent of the phenomenon is linearly proportional to the number of impacting particles, the fourth power of the impact velocity and the third power of the drop diameter.

$$V_m = cV^4 d^3 n_m \qquad \text{Eq. (2)}$$

Dashtkar et al. [29] pointed out that material quality and surface roughness also play an important role in the phenomenon. In case of material quality, it is mainly a decrease in hardness, while in the latter a higher degree of surface roughness causes greater erosion wear. Mohamed et al. [30] mentioned the use of other leading edge protection methods, such as in-mold coating, where components (e.g., epoxy, polyester) are mixed into the material itself to increase its resistance. In case of post-mold coatings, a protective layer is applied in the form of a spray or paint. The article highlights polyurethane having an excellent resistance to erosion and sees great potential for erosion reduction through nanoparticles in the material structure.

This phenomenon also poses a major challenge for helicopter rotor designers, as these vehicles can often operate in heavy rain and sandstorms. To create wear-resistant blades, Weigel [31] investigated 74 different structural and material qualities of coatings specifically designed to protect against raindrop impact.

Steam turbines also exhibit erosion. Ahmad et al. [32] describes how steam, which expands continuously, can already appear as a liquid on the last blade rows, and its collision with the rotating blades causes erosion. The extent of erosion is primarily linked to the speed of collision, and the size of water droplets. Similar conclusions were reached by Gruttola et al. [33].

Regarding installed gas turbines, research of Surendran et al. [34] highlighted the improvement of the isentropic efficiency of compression by the introduction of water droplets, thus reducing the energy consumption of the plant. Their measurements have demonstrated that the presence of water results in lower polytropic displacement during compression, so that the pressure ratio can be increased to a greater extent for the same energy input. Thus, the protection of the blades from LEE becomes more essential.

At the earlier mentioned and described areas, the spinning wheels relatively allow rotating speeds compared to the followings, but it's important to note, that due to the relatively big sizes, the circumferential speeds can be high, that's why the water droplet erosion is so significant. Aircrafts with jet engines are also often exposed to weather conditions that can damage the propulsion system when it encounters different forms of water. Rain droplets and ice crystals can cause damage to the blades of the compression stages and can also affect the combustion process, according to Murthy [35]. Another aspect is the aircraft part materials chosen because of the trade-off—mentioned by Tobin et al. [36]—between the properties to allow the transmission and reception of radar signals and their typically lower erosion resistance.

Wittmann et al. [37] also detected WDE in a fuel cell turbocharger investigation. The erosion craters were limited to a vertical strip of the side of the suction and it was very

FIGURE 8 Leading edge erosion (LEE) of a wind turbine. Data taken from Ref. [29].

FIGURE 9 Water droplet erosion on a fuel cell turbocharger's turbine blade. Data taken from Ref. [37].

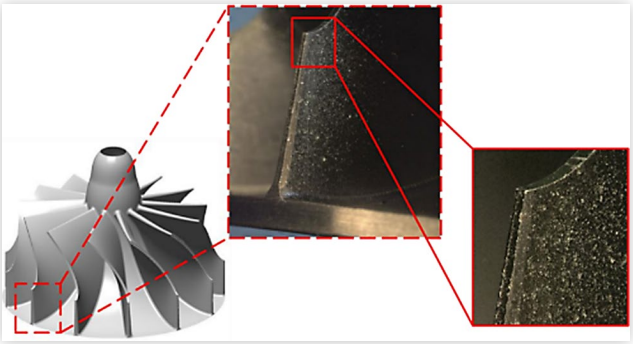

close to the leading edge. From here in the direction of flow, the number and size of impact craters decreased as shown in Figure 9.

Karstadt et al. [38] has extensively studied the effects of this phenomenon on turbochargers. He found that the formation of condensate water in the LP-EGR duct for turbochargers, as described earlier, is a function of the following engine parameters:

- Temperature of the ambient air
- Humidity of the ambient air
- Amount of ambient fog
- LP-EGR ratio
- Current load case of the engine

Not only does the collision of water particles with the impeller and the resulting blade abrasion reportedly cause a reduction in isentropic efficiency, but high speeds (up to 200,000 rpm) can easily cause the entire rotor assembly to become unbalanced, leading to unwanted acoustic noise or even failure of the entire assembly. Therefore, it is extremely important to investigate this area.

As detailed by Rieger et al. [39], the extent of damage to the compressor wheel is indicated by the following factors:

- Impact velocity
- Volume flow of the condensed water
- Impact angle
- Diameter of the water droplets (Figure 10)

In their component test bench experiments, they investigated the effect of these factors (shown in Figure 11), distinguishing between wall flow and free radius collision cases. Under certain conditions, the former caused the blade edges to buckle, and the latter caused the blade frontal surface to buckle. When varying the size of the water droplets it was shown that an increase in size in the 100–470 µm range leads to increasing erosion coefficient, but no significant change was detected above this size level at a given rotational speed over a given unit time, as shown in Figure 8.

A more precise assessment of erosion damage was carried out by electron microscopy, which showed that the wear was largely due to mechanical impact and to a lesser extent to chemical corrosion.

FIGURE 10 Influencing factors of water droplet erosion: (a) droplet speed and water column; (b) impact angle and the duration of the impact; (c) droplet diameter and water column. Data taken from Ref. [39].

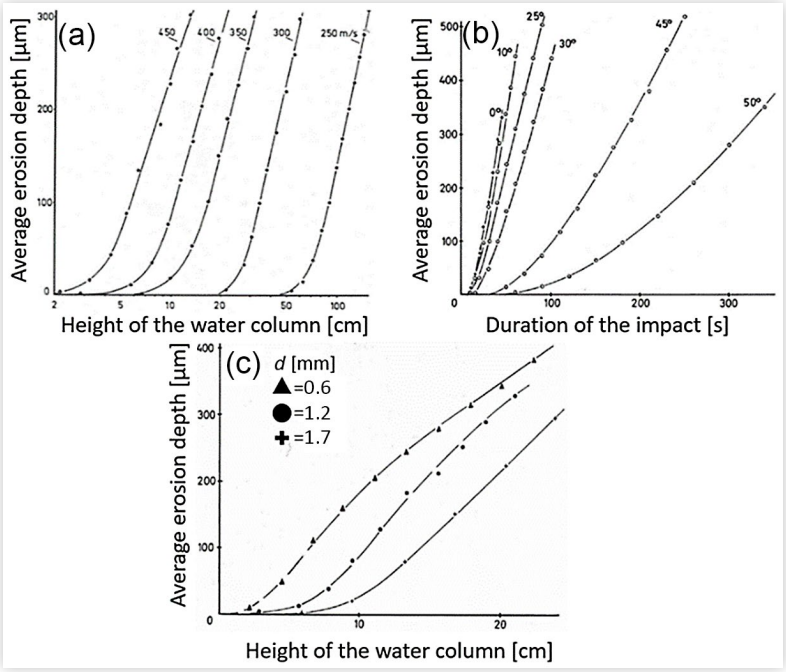

FIGURE 11 Erosion effect of different water droplet sizes. Data taken from Ref. [38].

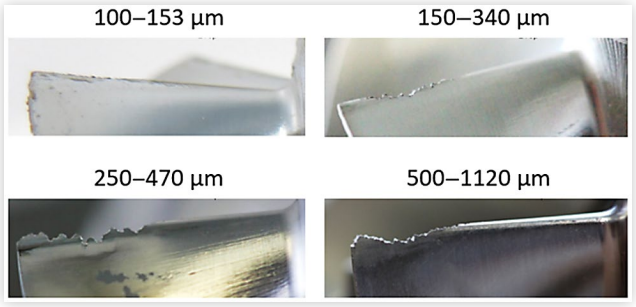

As mentioned in the introduction of [39], the phenomenon of wear can cause both serious acoustic and rotor dynamic problems, the latter of which has been investigated by vibration measurements. It was found that despite the damage, turbocharger vibration amplitudes remained below the maximum specified value.

Measurements were also carried out to investigate the isentropic efficiency of the compressor, which showed that the evaporative enthalpy of the condensate present removes heat from the compression process, thus increasing the value of this characteristic, but resulting in a lower isentropic efficiency due to the damage, which may negatively affect the volumetric efficiency of the engine.

As a further test case, the speed of the compressor was varied at the same water particle size and flow rate, which revealed that no significant damage occurs below a certain speed, while increasing the speed results in more severe damage and wear. However, no mathematical function for this relationship has been defined.

To protect the blades, a coating layer was developed, which showed excellent resistance to erosion, but no chemical or structural explanation was given.

Castorrini et al. [28] investigated the threshold damage velocity (v_D) and defined the following formula:

$$v_D \sim 1.41\left(\frac{K_m^2 c_m}{\rho_w^2 c_w^2 d_w}\right)^{1/3} \qquad \text{Eq. (3)}$$

where ρ_w and c_w are the density of the water and the compressional wave speed in water, d_w is the droplet diameter, K_m is the fracture toughness of the target material, and c_m is the Rayleigh wave velocity of the target material.

Galindo et al. [40] showed that under specific operation conditions, the condensation is present for up to 10 minutes after a cold start. This has a significant impact on the lifetime of the compressor.

Serrano et al. [41] defined an equation in which the dew point temperature T_{dew} can be calculated from the relative humidity and ambient temperature as follows:

$$T_{dew} = \sqrt[8]{\frac{RH}{100}}\left(112+0.9T\right)+\left(0.1T\right)-112 \qquad \text{Eq. (4)}$$

where T is the ambient temperature, RH is the relative humidity.

The amount of water condensate produced is determined in most of the literature by testing. However, several analytical methods have been developed by Nyerges et al. [42] to obtain the desired value in a time and cost-effective manner, such as the "Estimation by the engine volumetric efficiency and by the oxygen mass fraction changes."

Other important factors influencing the extent of damage are the hardness of the material and the surface roughness, according to the research of Kirols [43]. The latter mainly affects the length of the incubation period, while the former is directly proportional to erosion resistance raised to the power of 2.5.

3. Solutions to Simulate Condensation and Damage

Nowadays, the use of simulation methods is essential in a development process. However, it is not only a question of representing reality as accurately as possible, but also of creating complex mathematical and physical models that would be difficult or impossible to test in real life.

The condensation phenomenon mentioned in the previous chapter and the process of compressor wheel deterioration fall into this category. An example was demonstrated in the research of Galindo et al. [44] using Star CCM+ software with a simplified model, where two throttle valves were placed in the intake system, one at the beginning of the LP-EGR duct and another in front of the mixing point of the recirculated exhaust gas and air from the environment. Different angular positions of the implemented throttle valves cause different degrees of turbulence, with an increase in turbulence leading to a higher degree of condensation. The phenomenon depends on the temperature and humidity of the ambient air and recirculated exhaust gas, and it is also important to consider the corresponding pressure values.

The article also identifies the section after the LP-EGR cooler, and after the LP-EGR and intake duct junction as potential locations for condensation, especially in cold starts with cold intake ambient air temperatures.

It's important to mention that the purpose of Galindo's model is focusing on the root reason (condensed droplets collision) of WDE instead of wear prediction.

Specifically for the study of water droplet erosion (WDE), Andreoli et al. [45] developed a simulation model that can predict and describe the damage process more accurately than previous models (e.g., Springer's model), by considering the hardness and surface roughness of the material. The process is characterized by three stages illustrated in Figure 12 as a function of the amount of water in contact.

Andreoli denotes the aforementioned stages as:

I. Incubation period where surface roughness increases with no material loss (generation of micro-cracks)

FIGURE 12 WDE curve. Data taken from Ref. [45].

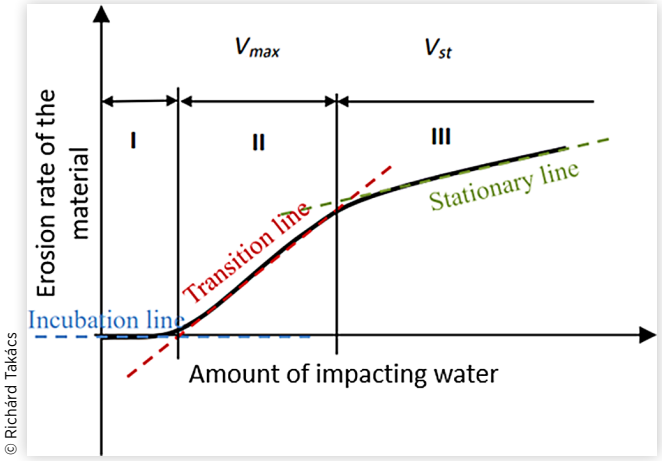

II. Transitional period in which the erosion rate (V) increases to its maximum V_{max}, whose value is kept for a certain time, and then decreases

III. Steady-state period with constant erosion rate (V_{st})

He also identifies the size of the water droplets as the main parameter influencing the extent of damage and proposes a mathematical description in the following forms:

- Models based on the similarity between fatigue damage and erosion process
- Models linking the erosion damage to the amount of energy applied to the surface
- Models entirely based on experimental data

For 20Kh13 steel as a base material, Seleznev et al. [46] calculated the erosion rate by varying the velocity of the impacting particle and its diameter in a series of measurements. The results are in agreement with the practical conclusions of [38], but present full curves of erosion instead of working points. The effect of the magnitude of these two parameters and the amount of water on erosion are also clearly shown in Figure 13.

Eisenberg et al. [47] used several sources and models to develop an analytical formula for calculating the number of impacts required to initiate damage (N_i).

$$N_i = \frac{8.9}{d^2}\left(\frac{S}{P}\right)^{5,7} \quad \text{Eq. (5)}$$

The magnitude of the above parameter is inversely proportional to the square of the diameter of the impacting particles (d), as well as with the (P), and directly proportional to the hardness of the material (S).

In their study, Chaboche and Lemaitre [48] highlighted that for a precise erosion prediction model due to water droplet impact, a time- and temperature-dependent plasticity model must be implemented for the eroded solid material.

FIGURE 13 Curves of erosion wear for 20Kh13 steel at different collision velocities and droplet diameters. Data taken from Ref. [46].

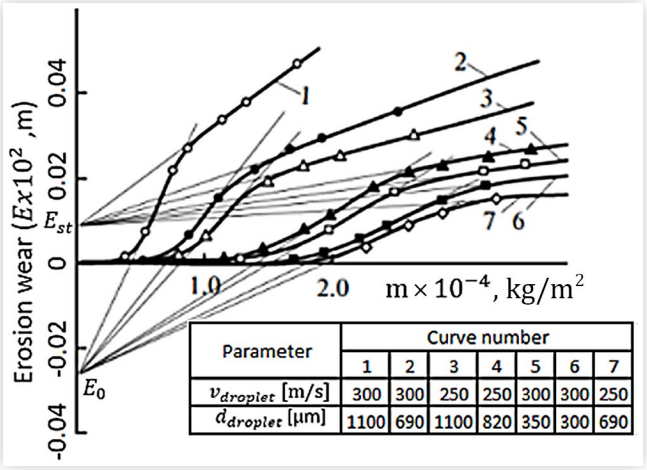

Parameter	Curve number						
	1	2	3	4	5	6	7
$v_{droplet}$ [m/s]	300	300	250	250	300	300	250
$d_{droplet}$ [μm]	1100	690	1100	820	350	300	690

4. Material Technology, Coatings, and Other Solutions to Reduce WDE

The protection of wind turbines, steam turbines, and other industrial rotor's LEE is also a widely investigated area. Most of the researchers defined two different categories of protection, namely the in-mold and the post-mold techniques. The first one applies a coating layer of similar material as the base matrix material (polyurethane, epoxy, polyester) in the mold during the manufacturing process, while the post-mold solution uses rollers or spray to apply a flexible coating on the surface. Regarding Herring et al. [49], the former method has an advantage of no additional step in the manufacturing process (which means a lower cost solution at the same time), while the latter is more ductile and have a low impedance. Leading edge protection tapes also provide a possible solution, but Amirzadeh et al. [50] showed that they can degrade the aerodynamic performance.

In his study—made with martensitic stainless steel and Ti6Al4V—Kirols et al. [51] described a practical tool to delay the WDE by improving the final surface quality and by reducing the initial surface roughness of the base material. Compared to the coating techniques, this means a lower cost solution, but it could be more difficult to implement it on complex surfaces. Mahdipoor et al. [52] studied and reached good results with a so-called high-velocity oxygen fuel (HVOF) sprayed coating technique for the same purpose. This methodology uses injected oxygen in a (combustion chamber where the melting heat generated from the ignition and the momentum of propulsion of the particles into the substrate. They used this type of coating on WC-12Co material with different microstructures. They

found a correlation between the WDE resistance and the microstructure of the coating, that's why the spraying process must be well controlled. The main advantages of this technique compared to other thermal spray processes are the higher strength bond to the underlying substrate and improved cohesive strength within the coating, smoother as-sprayed surface due to higher impact velocities and smaller powder sizes and thicker coating due to less residual stresses. However, HVOF spraying requires experienced, qualified personnel to ensure safe operation and to achieve consistent coating quality and the powder sizes are restricted to a range of about 5–60 µm, with a need for narrow size distributions.

There are only a few literatures on the avoidance of water particle collisions in turbochargers. A possible geometrical solution could be right choice of the mixing flow field area, but there are only a few existing solutions published. Although, Galindo et al. [53] demonstrated that a careful design of the LP-EGR and fresh air connection can prevent the mixing between streams from happening, which results in a limited interaction to a thin surface and thus the condensation can be reduced significantly, Reihani et al. [19] concluded that it has a high effect on the compressor isentropic efficiency, mainly at higher rates of EGR. However, the exhaust emission trends mentioned in the introduction call for the use of increasingly higher LP-EGR ratios, which may result in higher water condensate concentrations and thus higher levels of damage or damage before the design time. Due to the high operating speed range, the low weight of the structure, and the low rotor inertia to achieve a dynamic gas reaction, turbocharger impellers are usually made of aluminum alloy due to their low specific weight. Common alloying elements are copper, magnesium, and nickel. Today, the development of 3D printing and the major advances in plastic manufacturing technology have made it possible to research a version of the impeller manufactured through additive technologies. However, Andrearczyk et al. [54] showed that the use of materials manufactured by this technology does not always fulfill the mechanical requirements appearing on the compressor side of the turbocharger. Although considerable advantages can be achieved in terms of rotor dynamics (improved flow properties, better gas response, higher mechanical efficiency), the M3 X polymerics' thermal load capacity and the maximum speed at which it can be used are also limited. The latter has also been verified by the author using a vibration measurement method, where it has been shown that above 100,000 rpm the deflection can be larger than the gap between the compressor wheel and the surrounding housing. Mechanical contact between these parts can even cause the entire structure to fail. However, recirculating the exhaust gas to the compressor required solving several problems while using this grade of material. For unfiltered direct injection gasoline engines as well as for diesel engines in a certain size range, the effect of particulate abrasion must be considered. In addition, improvements are needed to avoid erosion caused by water condensate as discussed earlier. Münz et al. [55] also attributed a corrosive effect to the pollutants and strong acids generated in this part of the exhaust system. Song et al. [56] attempted to achieve a reduction in condensation with the same NO_x emissions without geometric modifications, simply by optimizing the HP-EGR and LP-EGR control strategies. Using GT-Power software, a light-duty diesel engine and a corresponding condensation model were created and validated. In the end, a 34% reduction in condensation was achieved during a Worldwide Harmonized Light Vehicles Test Cycle (WLTC) cycle at 23°C ambient air temperature, but with a ~1% increase in brake specific fuel consumption (BSFC). The rationale is that, for the same NO_x emissions, a reduction in LP-EGR volume results in a larger increase in HP-EGR (the latter having a lower NO_x reducing efficiency), which overall results in a larger amount of EGR, reduced engine efficiency, and thus higher BSFC levels.

5. Detecting Damage on the Compressor Wheel

The individual elements of the turbocharger rotor have different natural frequencies, which can become resonant due to the excitation caused by the speed of rotation, which can lead to damage and failure. Research by Zheng et al. [57] shows that this phenomenon is particularly relevant for large impeller blades, where the natural frequency ranges could be the same as the excitation frequency. The erosion caused by fluid impact is also manifested as altered vane pass noise. Detection of this phenomenon can provide important information about the current state of the impeller.

Serrano et al. [58] developed a solution for visual observation in their research. A high-speed camera was used to capture thousands of images per second, which provides important information on the positioning of the contact point(s) of the compressor wheel and the material/medium it is colliding with, as well as on the flow pattern of the medium. In addition to several different materials (e.g., air filter piece, M6 nut, suction pipe piece), ice crystals, condensate, and blow-by particles in liquid form were also impacted. Vibration measurements were also carried out to detect the extent of damage. Furthermore, thermodynamic characteristics were also monitored in order to refer to the level of damage from the temperature change at the compressor outlet. They found that minor or early damage can be detected more accurately by the vibration measuring method, while the thermodynamic method also plays a significant role in the case of major damage.

For online condition monitoring, Sandoval et al. [59] used the method of vibration measurement and acoustic noise detection, with the aim to avoid complete failure of the compressor wheel under real-life conditions. They manually recreated some typical failures and investigated the effects of them using 20 kHz sampling frequency from three orthogonal vibration sensors' signal and fast Fourier transformation for the signal processing. They detected an increase in the vibration levels on the frequency range from 1.5 kHz to 3 kHz

during the operational failure tests, but they did not give a deeper explanation about the reason and suggested further investigations.

In their research, Li et al. [60] used a pressure pulsation sensor placed near to the expected crack area of a centrifugal compressor blade and inferred to the damage from the corresponding casing vibration signals. They described also that these signals itself cannot show a direct correlation to the damage, but combining the process with the so-called squared envelope spectrum method gives the possibility for condition monitoring.

Considering the same propulsion power of the turbine, the appearance of the compressor wheel damage due to WDE can be detected from the change in the turbocharger's speed also, according to Marieta's research [61]. The reason is the changed air transport capacity of the damaged compressor.

6. Summary: Key Insights of Influencing Factors, Mitigation Strategies, and Detection Methods for WDE

The following general observations can be made based on the findings of this article:

- WDE is still of great importance in many engineering fields (wind turbine, steam turbines, helicopter rotor, fuel cell, aircraft). In case of turbochargers, the damaging effect of this phenomenon is caused by the high-velocity collision of water condensed in the low-pressure exhaust gas recirculation system with rotating vanes, the typical impact angle, and the inadequate material structure and surface parameters.
- The amount of wear volume by time caused by WDE is linearly proportional to the number of impacting particles, the 4th power of the impact velocity, and the 3rd power of the drop diameter in case of spinning wheels with larger size and relatively lower speed. At the range of smaller wheels with higher speed these parameters are taking into account with a power of 5–5.2 and a power of 2. Other influencing factors are the impact angle, the hardness, the ductility, fracture toughness, and fatigue limit of the raw material and its surface roughness.
- The rate of wear over time for the same water flow rate is described by the WDE curve, which has the following stages: incubation time, transition time, stationary time.
- The use of different types of coating techniques such as in-mold and post-mold technique (sol-gel thin film, gelcoat, polyurethane-based surface coatings) have proven to decrease erosion in wind turbine applications and pointed out that without these, aerodynamic performance loss can be as high as 20–25%.
- Regarding damage detection cause by erosion, the available methods can be split into two categories:
  - "In situ" early detection through acoustic/vibroacoustic measurements, high-speed videography, or through monitoring indirectly related parameters, such as the isentropic efficiency of a compressor.
  - "Postmortem" detection through visual inspection, optical microscopy, or scanning electron microscopy.
- The LP-EGR system has a huge potential in NO_x emission reduction for both gasoline and diesel engines. The biggest drawback of this system is the appearance of condensed water. The amount of it is depending on the humidity and temperature of the intake air, the EGR ration, and the current load case of the engine. Cold start and high brake mean effective pressure in the low-speed range are considered as critical load cases.
- Important viewpoints and results of WDE at turbocharger research:
  - Several authors [20, 37, 40, 44] have successfully developed 3D CFD simulations for modeling the water condensation phenomenon showing good correlation with real physical measurements, but there is a lack of modeling WDE prediction on compressor blades.
  - Karstadt et al. [38] has shown that the amount of erosion on compressor blades depends on:
    - Compressor speed: no significant damage occurs below a certain speed, while increasing the speed results in more severe damage and wear.
    - Droplet diameter: increase in size in the 100–470 µm range leads to increasing erosion coefficient, but no significant change was detected above this size level at a given rotational speed over a given unit time.
    - Angle of collision: the higher the angle of collision the higher the detected erosion.
- There are several potentials for future developments regarding turbocharger WDE investigation and protection such as (author's opinion based on literature review):
  - Simulation of wear and lifetime prediction of different compressor wheels.
  - Investigation of different compressor wheel materials with different levels of hardness and surface roughness.
  - Definition of protecting techniques such as chemical composition, coatings.
  - Development of a vibration system, which can accurately monitor the level of damage.

Acknowledgements

Project no. TKP2021-NVA-23 has been implemented with the support provided by the Ministry of Technology and Industry of Hungary from the National Research, Development and Innovation Fund, financed under the TKP2021-NVA funding scheme. This article is also supported by the ÚNKP-23—New National Excellence Program of the Ministry for Culture and Innovation from the Source of the National Research, Development and Innovation Fund. This article is published in the framework of the project "Production and Validation of Synthetic Fuels in Industry-University Collaboration," project number ÉZFF/956/2022-ITM_SZERZ.

Contact Information

Richárd Takács, corresponding author
Széchenyi István University
takacs.richard@sze.hu
ORCID: 0000-0002-2223-2123

Abbreviations

BSFC - Brake specific fuel consumption
c_m - Rayleigh wave velocity
c_w - Density of the water
d - Diameter of the droplet
d_{ref} - Reference diameter of the droplet
E - Erosion rate
EGR - Exhaust gas recirculation
HP-EGR - High-pressure exhaust gas recirculation
HSDI - High-speed direct injection
HV - Hardness Vickers
HVOF - High-velocity oxygen fuel
ICE - Internal combustion engine
k - Erosion rate constant
K_m - Fracture toughness of the target material
LEE - Leading edge erosion
LP-EGR - Low-pressure exhaust gas recirculation
m - Droplet mass flow rate
m_{ref} - Reference droplet mass flow rate
NEDC - New European driving cycle
N_i - Number of impacts
n_m - Number of impacting particles
P - Pressure of impact
RH - Relative humidity
S - Hardness of the material
SEM - Scanning electron microscope
T - Temperature
T_{dew} - Dew temperature
V - Impact velocity of the droplet
V_D - Threshold damage velocity
V_{ref} - Reference impact velocity
WDE - Water droplet erosion
WLTC - Worldwide Harmonized Light Vehicles Test Cycle
ρ_w - Density of the water

References

1. Del Pero, F., Delogu, M., and Pierini, M., "Life Cycle Assessment in the Automotive Sector: A Comparative Case Study of Internal Combustion Engine (ICE) and Electric Car," *Procedia Structural Integrity* 12 (2018): 521-537.
2. BP Statistical Review of World Energy 2022, "Statistical Review of World Energy 2022," accessed August 31, 2023, www.bp.com.
3. Serrano, J.R., Novella, R., and Piqueras, P., "Why the Development of Internal Combustion Engines is Still Necessary to Fight Against Global Climate Change from the Perspective of Transportation," *Applied Sciences* 9 (2019): 4597, doi:https://doi.org/10.3390/app9214597.
4. European Commission, "European Commission: Note on the Application of Regulation (EU) 2017/1151 as Amended by Regulation (EU) 2018/1832," Industrial Transformation and Advanced Value Chains, Automotive and Mobility Industries, Brussels, 2019.
5. Nowak, M., Walkowski, D., and Kubiak, Sz., "In Principle: New Emission Standards," February 25, 2021, accessed February 25, 2023, https://codozasady.pl/en/p/new-emission-standards.
6. Seykens, X., Kupper, F., Mentink, P., and Ramesh, S., "Towards Ultra-Low NO_x Emissions within GHG Phase 2 Constraints: Main Challenges and Technology Directions," SAE Technical Paper 2018-01-0331 (2018), doi:https://doi.org/10.4271/2018-01-0331.
7. Venu, H., Subramani, L., and Raju, D.V., "Emission Reduction in a DI Diesel Engine Using Exhaust Gas Recirculation (EGR) of Palm Biodiesel Blended with TiO_2 Nano Additives," *Renewable Energy* 140 (2019): 245-263, doi:https://doi.org/10.1016/j.renene.2019.03.078.
8. Luján, M.J., Pla, B., Moroz, S., and Bourgoin, G., "Acidic Condensation in Low Pressure EGR Systems Using Diesel and Biodiesel Fuels," *SAE Int. J. Fuels Lubr.* 2, no. 2 (2010): 305-312, doi:https://doi.org/10.4271/2009-01-2805.

9. Bermúdez, V., Lujan, M.J., Pla, B., and Linares, G.W., "Effects of Low Pressure Exhaust Gas Recirculation on Regulated and Unregulated Gaseous Emissions during NEDC in a Light-Duty Diesel Engine," *Energy* 36 (2011): 5655-5665.
10. Lapuerta, M., Ramos, Á., Fernández-Rodríguez, D., and González-García, I., "High-Pressure versus Low-Pressure Exhaust Gas Recirculation in a Euro 6 Diesel Engine with Lean-NO_x Trap: Effectiveness to Reduce NO_x Emissions," *International Journal of Engine Research* 20, no. 1 (2019): 155-163, doi:https://doi.org/10.1177/1468087418817447.
11. Ladommatos, N., Abdelhalim, M.S., Zhao, H., and Hu, Z., "Effects of EGR on Heat Release in Diesel Combustion," in *International Congress and Exposition*, Detroit, MI, February 23–26, 1998.
12. Jung, D., Hwang, I., Jo, Y., Jang, C. et al., "In-Cylinder Pressure-Based Convolutional Neural Network for Real-Time Estimation of Low-Pressure Cooled Exhaust Gas Recirculation in Turbocharged Gasoline Direct Injection Engines," *International Journal of Engine Research* 22, no. 3 (2021): 815-826, doi:https://doi.org/10.1177/1468087419879002.
13. Serrano, J.R., Piqueras, P., Navarro, R., Tarí, D. et al., "Development and Verification of an In-Flow Water Condensation Model for 3D-CFD Simulations of Humid Air Streams Mixing," *Computers and Fluids* 167 (2018): 158-165.
14. Desantes, J.M., Luján, J.M., Pla, B., and Soler, J.A., "On the Combination of High-Pressure and Low-Pressure Exhaust Gas Recirculation Loops for Improved Fuel Economy and Reduced Emissions in High-Speed Direct-Injection Engines," *International Journal of Engine Research* 14, no. 1 (2013): 3-11.
15. Warey, A., Bika, A.S., Long, D., Balestrino, S. et al., "Influence QOF Water Vapor Condensation on Exhaust Gas Recirculation Cooler Fouling," *International Journal of Heat and Mass Transfer* 65 (2013): 807-816, doi:https://doi.org/10.1016/j.ijheatmasstransfer.2013.06.063.
16. Siokos, K., Koli, R., Prucka, R., Schwanke, J. et al., "Assessment of Cooled Low Pressure EGR in a Turbocharged Direct Injection Gasoline Engine," *SAE Int. J. Engines* 8, no. 4 (2015): 1535-1543, doi:https://doi.org/10.4271/2015-01-1253.
17. Dimitriou, P., Turner, J., Burke, R., and Copeland, C., "The Benefit of a Mid-Route Exhaust Gas Recirculation System for Two-Stage Boosted Engines," *International Journal of Engine Research* 19, no. 5 (2018): 553-569, doi:https://doi.org/10.1177/1468087417723782.
18. Galindo, J., Dolz, V., Monsalve-Serrano, J., Maldonado, M.A.B. et al., "Advantages of Using a Cooler Bypass in the Low-Pressure Exhaust Gas Recirculation Line of a Compression Ignition Diesel Engine Operating at Cold Conditions," *International Journal of Engine Research* 22, no. 5 (2021): 1624-1635, doi:https://doi.org/10.1177/1468087420914725.
19. Reihani, A., Hoard, J., Klinkert, S., Kuan, C. et al., "Experimental Response Surface Study of the Effects of Low-Pressure Exhaust Gas Recirculation Mixing on Turbocharger Compressor Performance," *Applied Energy* 261 (2020): 114349, doi:https://doi.org/10.1016/j.apenergy.2019.114349.
20. Yudanov, M., "Novel Turbo Compressor System with Liquid Erosion Resistance for a DME Truck," Master's thesis, Department of Applied Mechanics, Chalmers Technical University Gothenburg, Gothenburg, 2016.
21. Heymann, F.J., "Liquid Impingement Erosion," *ASM Handbook, Friction, Lubrication and Wear Technology*, Ohio, vol. 18 (1992), 221-231.
22. Amirzadeh, B., Louhghalam, A., Raessi, M., and Tootkaboni, M., "A Computational Framework for the Analysis of Rain-Induced Erosion in Wind Turbine Blades, Part I: Stochastic Rain Texture Model and Drop Impact Simulations," *Journal of Wind Engineering and Industrial Aerodynamics* 160 (2017): 33-43, doi:https://doi.org/10.1016/j.weia.2016.12.007.
23. Li, N., Zhou, Q., Chen, X., Xu, T. et al., "Liquid Drop Impact on Solid Surface with Application to Water Drop Erosion on Turbine Blades, Part I: Nonlinear Wave Model and Solution of One-Dimensional Impact," *International Journal of Mechanical Sciences* 50 (2008): 1526-1542.
24. Hammitt, F.G., Huang, Y.C., Kling, C.L., Mitchell, T.M. Jr. et al., *A Statistically Verified Model for Correlating Volume Loss due to Cavitation or Liquid Impingement, Characterization and Determination of Erosion Resistance*. Vol. 474 (ASTM International, University of Michigan, 1970), 288-322.
25. Hattori, S. and Kakuichi, M., "Effect of Impact Angle on Liquid Droplet Impingement Erosion," *Wear* 298-299 (2013): 1-7, doi:https://doi.org/10.1016/j.wear.2012.12.025.
26. ASTM, "Standard Test Method for Liquid Impingement Erosion Using Rotating Apparatus," ASTM G73-10, ASTM International, West Conshohocken, PA, 2010, www.astm.org.
27. Chen, J., Wang, J., and Ni, A., "A Review on Rain Erosion Protection of Wind Turbine Blades," *Journal of Coatings Technology Research* 16 (2019): 15-24, doi:https://doi.org/10.1007/s11998-018-0134-9.
28. Castorrini, A., Corsini, A., Rispoli, F., Venturini, P. et al., "Computational Analysis of Wind-Turbine Blade Rain Erosion," *Computers and Fluids* 141 (2016): 175-183, doi:https://doi.org/10.1016/j.compfluid.2016.08.013.
29. Dashtkar, A., Hadavinia, H., Sahinkaya, M.N., Williams, N.A. et al., "Rain Erosion-Resistant Coatings for Wind Turbine Blades: A Review," *Polymers and Polymer Composites* 27, no. 8 (2019): 443-475, doi:https://doi.org/10.1177/0967391119848232.
30. Mohamed, E.I. and Mamoun, M., "Water Droplet Erosion of Wind Turbine Blades: Mechanics, Testing, Modeling and Future Perspectives," *Materials* 13, no. 1 (2020): 157, doi:https://doi.org/10.3390/ma13010157.
31. Weigel, W.D., "Advanced Rotor Blade Erosion Protection System," Aviation Applied Technology Directorate U.S. Army Aviation and Troop Command, Fort Eustis, VA, 1996.
32. Ahmad, M., Schatz, M., and Casey, M.V., "Experimental Investigation of Droplet Size Influence on Low Pressure Steam Turbine Blade Erosion," *Wear* 303 (2013): 83-86.

33. Di Gruttola, F., Agati, G., Venturini, P., Borello, D. et al., "Numerical Study of Erosion due to Online Water Washing in Axial Flow Compressors," in *Turbomachinery Technical Conference and Exposition GT2020*, London, England, June 22–26, 2020.
34. Surendran, A. and Kim, H.D., "Effects of Wet Compression on the Flow Behavior of a Centrifugal Compressor: A CFD Analysis," in *Proceedings of ASME Turbo Expo 2014: Turbine Technical Conference and Exposition GT2014*, Düsseldorf, Germany, June 16–20, 2014.
35. Murthy, S.N.B., "Effect of Atmospheric Water Ingestion on the Performance and Operability of Flight Gas Turbines," American Institute of Aeronautics and Astronautics Inc., 1996, doi:https://doi.org/10.2514/6.1996-3059.
36. Tobin, E.F., Young, T.M., Raps, D., and Rohr, O., "Comparison of Liquid Impingement Results from Whirling Arm and Water-Jet Rain Erosion Test Facilities," *Wear* 271 (2011): 2625-2631.
37. Wittmann, T., Lück, S., Bode, C., and Friedrichs, J., "Investigation of Water Droplet Erosion in the Radial Turbine of a Fuel Cell Turbocharger," in *Proceedings of Global Power and Propulsion Society*, Virtual, October 18–20, 2021.
38. Karstadt, S., Werner, J., Münz, S., and Aymanns, R., "Effect of Water Droplets Caused by Low Pressure EGR on Spinning Compressor Wheels," in *19th Supercharging Conference*, Dresden, Germany, 2014.
39. Rieger, H., "Kavitation und Tropfenschlag," in Machenrauch, E. and Gerold, V. (eds.), *Beiträge zur Werkstoffkunde und Werkstofftechnik* (Karlsruhe, Germany: Werkstofftechnische Verlagsgesellschaft m.b.H., 1977).
40. Galindo, J., Navarro, R., Tarí, D., and Moya, F., "Development of an Experimental Test Bench and a Psychrometric Model for Assessing Condensation on a Low-Pressure Exhaust Gas Recirculation Cooler," *International Journal of Engine Research* 22, no. 5 (2021): 1540-1550, doi:https://doi.org/10.1177/1468087420909735.
41. Serrano, J.R., Piqueras, P., Angiolini, E., Meano, C. et al., "On Cooler and Mixing Condensation Phenomena in the Long-Route Exhaust Gas Recirculation Line," SAE Technical Paper 2015-24-2521 (2015), doi:https://doi.org/10.4271/2015-24-2521.
42. Nyerges, Á. and Zöldy, M., "Verification and Comparison of Nine Exhaust Gas Recirculation Mass Flow Rate Estimation Methods," *Sensors* 20 (2020): 7291, doi:https://doi.org/10.3390/s20247291.
43. Kirol, H.S., "Water Droplet Erosion: Influencing Parameters, Representation and Comparison," Masters thesis, Master of Applied Science, Concordia University Montreal, Canada, 2015.
44. Galindo, J., Navarro, R., Tarí, D., and García-Olivas, G., "Centrifugal Compressor Influence on Condensation due to Long-Route Exhaust Gas Recirculation Mixing," *Applied Thermal Engineering* 144 (2018): 901-909.
45. Andreoli, M., Gabriele, S., Venturini, P., and Borello, D., "New Model to Predict Water Droplets Erosion Based on Erosion Test Curves, Application to On-Line Water Washing of a Compressor," in *Proceedings of ASME Turbo Expo. Turbomachinery Technical Conference and Exposition*, Phoenix, AZ, 2019, doi:https://doi.org/10.1115/GT2019-92033.
46. Seleznev, L.I., Ryzhenkov, V.A., and Mednikov, A.F., "Phenomenology of Erosion Wear of Constructional Steels and Alloys by Liquid Particles," *Thermal Engineering* 57, no. 9 (2010): 741-745, doi:https://doi.org/10.1134/S004060151009003X.
47. Eisenberg, D., Laustsen, S., and Stege, J., "Wind Turbine Blade Coating Leading Edge Rain Erosion Model: Development and Validation," *Wind Energy* 21 (2018): 942-951, doi:https://doi.org/10.1002/we.2200.
48. Chaboche, J.L. and Lemaitre, J., *Mechanics of Solid Materials* (Cambridge, UK: Cambridge University Press, 1995)
49. Herring, R., Dyer, K., Martin, F., and Ward, C., "The Increasing Importance of Leading Edge Erosion and a Review of Existing Protection Solutions," *Renewable and Sustainable Energy Reviews* 115 (2019): 109382.
50. Amirzadeh, B., Louhghalam, A., Raessi, M., and Tootkaboni, M., "A Computational Framework for the Analysis of Rain-Induced Erosion in Wind Turbine Blades, Part II: Drop Impact-Induced Stresses and Blade Coating Fatigue Life," *Journal of Wind Engineering and Industrial Aerodynamics* 163 (2017): 44-54, doi:https://doi.org/10.1016/j.weia.2016.12.007.
51. Kirols, H.S., Kevorkov, D., Uihlein, A., and Medraj, M., "The Effect of Initial Surface Roughness on Water Droplet Erosion Behaviour," *Wear* 342-343 (2015): 198-209, doi:https://doi.org/10.1016/j.wear.2015.08.019.
52. Mahdipoor, M.S., Tarasi, F., Moreau, C., Dolatabadi, A. et al., "HVOF Sprayed Coatings of Nano-Agglomerated Tungsten-Carbide/Cobalt Powders for Water Droplet Erosion Application," *Wear* 330-331 (2015): 338-347, doi:https://doi.org/10.1016/j.wear.2015.02.034.
53. Galindo, J., Navarro, R., Tarí, D., and Moya, F., "Quantitative Validation of an In-Flow Water Condensation Model for 3D-CFD Simulations of Three-Way Junctions Using Indirect Condensation Measurements," *International Journal of Thermal Sciences* 172 (2022): 107303, doi:https://doi.org/10.1016/j.ijthermalsci.2021.107303.
54. Andrearczyk, A., Baginski, P., and Klonowicz, P., "Numerical and Experimental Investigations of a Turbocharger with a Compressor Wheel Made of Additively Manufactured Plastic," *International Journal of Mechanical Sciences* 178 (2020): 105613, doi:https://doi.org/10.1016/j.ijmecsci.2020.105613.
55. Münz, S., Römuss, C., Schmidt, P., Brune, K.H. et al., "Dieselmotoren mit Niederdruck-Abgasrückführung Abgasrückführung," *MTZ-Motortechnische Zeitschrift* 69, no. 2 (2008): 124-130.

56. Song, H. and Song, S., "Numerical Investigation on a Dual Loop EGR Optimization of a Light Duty Diesel Engine Based on Water Condensation Analysis," *Applied Thermal Engineering* 182 (2021): 116064, doi:https://doi.org/10.1016/j.applthermaleng.2020.116064.

57. Zheng, W., Zengquan, W., Li, Z., and A-na, W., "Time-Dependent Vibration Frequency Reliability Analysis of Blade Vibration of Compressor Wheel of Turbocharger for Vehicle Application," *Chinese Journal of Mechanical Engineering* 27, no. 1 (2014): 205-210, doi:https://doi.org/10.3901/CJME.2014.01.205.

58. Serrano, C., Martínez, T.B.V., Gargar, K.L., and Bouffaud, F., "Study of the Effects on Turbocharger Performance Generated by the Presence of Foreign Objects at the Compressor Intake," *Experimental Techniques* 37, no. 2 (2011): 30-40, doi:https://doi.org/10.1111/j.1747-1567.2011.00795.x.

59. Sandoval, O.R., Machado, L.H.J., Hanriot, V.M., Troysi, F. et al., "Acoustic and Vibration Analysis of a Turbocharger Centrifugal Compressor Failure," *Engineering Failure Analysis* 139 (2022): 106447, doi:https://doi.org/10.1016/j.engfailanal.2022.106447.

60. Li, H., Zhang, X., and Xu, F., "Experimental Investigation on Centrifugal Compressor Blade Crack Classification Using the Squared Envelope Spectrum," *Sensors* 13 (2013): 12548-12563, doi:https://doi.org/10.3390/s130912548.

61. Monieta, J., "Fundamental Investigation of Marine Engines Turbocharger Diagnostic with Use Acceleration Vibration Signals," *AIP Conf. Proc.* 2029 (2018): 020044, doi:https://doi.org/10.1063/1.5066506.